



## Research Article

<https://doi.org/10.1631/jzus.B2300947>



# OX40 ligand promotes follicular helper T cell differentiation and development in mice with immune thrombocytopenia

Ziyin YANG\*, Lei HAI\*, Xiaoyu CHEN, Siwen WU, Yan LV, Dawei CUI<sup>✉</sup>, Jue XIE<sup>✉</sup>

Department of Blood Transfusion, The First Affiliated Hospital, Zhejiang University School of Medicine, Hangzhou 310003, China

**Abstract:** Immune thrombocytopenia (ITP) is a hemorrhagic autoimmune disease characterized by antibody-mediated platelet injury. ITP has complicated immunopathological mechanisms that need further elucidation. It is well known that the costimulatory molecules OX40 ligand (OX40L) and OX40 play essential roles in the immunological mechanisms of autoimmune diseases. Previously, we discovered that the expression of *OX40L* and *OX40* is significantly increased in the peripheral blood mononuclear cells (PBMCs) of ITP patients. In our present study, OX40L-induced follicular helper T (Tfh) cells exhibited an activated phenotype with elevated expression of inducible T-cell costimulator (ICOS), programmed cell death protein-1 (PD-1), and cluster of differentiation 40 ligand (CD40L) *in vitro*. Moreover, aberrant OX40L–OX40 expression might promote the Tfh1-to-Tfh2 shift *in vivo*, inducing the generation of autoantibodies by enhancing the helper function of Tfh cells for B lymphocytes in a mouse model, which might accelerate the progression of ITP. Additionally, signal transduction through the OX40L–OX40 axis might be related to the activation of tumor necrosis factor receptor-associated factor (TRAF)–nuclear factor- $\kappa$ B (NF- $\kappa$ B) and Janus kinase (JAK)–signal transducer and activator of transcription (STAT) signaling pathways. Overall, OX40L–OX40 signaling is proposed as a potential novel therapeutic target for ITP.

**Key words:** OX40; OX40 ligand (OX40L); Immune thrombocytopenia; Follicular helper T (Tfh) cell; B cell

## 1 Introduction

Immune thrombocytopenia (ITP) is a heterogeneous acquired disease characterized by antibody-mediated platelet injury and low baseline platelet counts (Mingot-Castellano et al., 2022). Epidemiological data showed that ITP affects 2 to 4 per 100 000 persons annually, with a total incidence rate of 10 in 100 000 individuals (Ghanima et al., 2021). Patients show an increased risk of skin bruising and bleeding. Besides, low platelet counts may result in internal bleeding, particularly intracranial bleeding, which can be severe and even life-threatening to ITP patients (Ghanima et al., 2021).

Currently, multiple therapeutic approaches are utilized for the clinical treatment of ITP, including thrombopoietin receptor agonists, rituximab, and splenectomy (Liu et al., 2023). However, some patients are unresponsive to multiple treatment regimens and ultimately develop refractory ITP with prolonged and severe thrombocytopenia (Liu et al., 2023). Therefore, it is important to further elucidate the pathogenesis of ITP and identify new targeted therapies for this disease.

Platelet destruction and the suppression of platelet production are aggravated by multiple humoral immune responses and immune cell abnormalities in ITP patients. It has been well recognized that the pathogenesis of ITP is associated with the production of antiplatelet autoantibodies (Chen et al., 2022). However, the exact underlying mechanisms of ITP remain unclear. Follicular helper T (Tfh) cells are a particular subset of cluster of differentiation 4-positive (CD4<sup>+</sup>) T cells, which can migrate to target points and produce multiple cytokines that promote the occurrence and development of autoimmune disorders (Chen et al., 2022). The percentage of Tfh cells is increased in B cell-related autoimmune

✉ Jue XIE, zyyyxj2011@zju.edu.cn

Dawei CUI, dawaicui@zju.edu.cn

\* The two authors contributed equally to this work

Jue XIE, <https://orcid.org/0000-0002-4270-671X>

Dawei CUI, <https://orcid.org/0000-0003-3840-1486>

Ziyin YANG, <https://orcid.org/0000-0001-8542-1688>

Lei HAI, <https://orcid.org/0000-0002-5474-5492>

Received Jan. 7, 2024; Revision accepted Feb. 15, 2024;  
Crosschecked Jan. 6, 2025; Published online Mar. 6, 2025

© Zhejiang University Press 2025

disorder patients, such as those with systemic lupus erythematosus (SLE), primary Sjögren's syndrome, and rheumatoid arthritis (RA), which exhibits features of a highly activated state (Pontarini et al., 2020; Caza et al., 2022; Sasaki et al., 2022; Wei and Niu, 2023). Another critical role of Tfh cells in autoimmune diseases is to support B lymphocyte differentiation and facilitate the production of high-affinity autoantibodies (Audia et al., 2014; Hernandez-Molina et al., 2021). Tfh cells highly express CXC chemokine receptor type 5 (CXCR5) and the classical Tfh-associated transcription factor B-cell lymphoma 6 (Bcl6), and typically secrete interleukin-21 (IL-21) and several important surface markers, including inducible T-cell costimulator (ICOS), programmed cell death protein-1 (PD-1), and the costimulatory molecule OX40 (Jensen et al., 2022).

OX40 is a promising therapeutic target for diverse T cell-mediated disorders (Iriki et al., 2023). In several animal models of autoimmune disease and infectious disease, an OX40 agonist was shown to ligate OX40 and convey signals to activate T cells, thereby facilitating T-cell activation and proliferation (Fu et al., 2020). Researchers revealed that treating lupus patients with soluble OX40 ligand (OX40L) enhanced the expression levels of multiple characteristic markers associated with Tfh cells in vitro. Moreover, in murine models, OX40L–OX40 interactions encourage CD4<sup>+</sup> T cells to accumulate in B-cell follicles and at the T–B boundary (Fu et al., 2020). The mechanism through which the OX40L–OX40 axis influences T-cell function is complex. OX40L–OX40 signals, via the tumour necrosis factor (TNF) receptor-associated factor (TRAF) family, nuclear factor- $\kappa$ B (NF- $\kappa$ B) pathway, and Janus kinase–signal transducer and activator of transcription (JAK–STAT) pathway, can expand the immune response in T-cell subsets (Fu et al., 2020; Zhao et al., 2022). We previously reported that the peripheral blood mononuclear cells (PBMCs) of ITP patients exhibited considerably higher messenger RNA (mRNA) levels of *OX40L* and *OX40* (Cui et al., 2019). However, the specific mechanism of OX40L–OX40 costimulation signals promoting the development of ITP is unclear.

In this study, we sought to determine the expansion and activation patterns of Tfh cells and their subset induced by the abnormal signal of the OX40L–OX40 axis in ITP, which will offer new insights into exploration the pathogenesis of ITP, providing a novel targeted therapy for this disease.

## 2 Methods

### 2.1 Animals

We obtained 8-week-old C57BL/6J wild-type (WT) female mice from Ziyuan Experimental Animal Technology Co., Ltd., Hangzhou, China. The animals were maintained under a 12-h light/dark cycle with a controlled temperature and were allowed to acclimate for one week before experimentation. All animal experiments were carried out based on the Guide for the Use and Care of Laboratory Animals, 8th Edition (National Research Council (US) Committee for the Update of the Guide for the Care and Use of Laboratory Animals, 2011).

### 2.2 Passive ITP model

Twenty female mice were equally divided into two groups: control group ( $n=10$ ) and ITP group ( $n=10$ ). Murine thrombocytopenia was induced and maintained as previously described (Sun et al., 2018): each mouse was intraperitoneally injected with 4  $\mu$ g/d agents (monoclonal platelet antibody (MWReg30) in 200  $\mu$ L of phosphate-buffered saline (PBS) at pH 7.2) for 7 d. Meanwhile, the control mice were treated with the same amount of PBS. Whole blood samples (5  $\mu$ L) were collected through the tail vein, mixed with diluents (V-3D, Mindray, Shenzhen, China), and collected in ethylene diamine tetraacetic acid (EDTA)-K2 tubes. The baseline platelet counts of the mice were determined before injection, and the platelet numbers were counted daily for 7 d after injection. Platelet counts were performed by an automatic hematology analyzer (BV-30Vet, Mindray).

### 2.3 Histopathological study and immunofluorescence assay

The mice were sacrificed after 7 d of injection and spleen tissues were harvested for histopathological analyses. Hematoxylin and eosin (H&E) staining, immunohistochemical (IHC) staining, and immunofluorescence staining, as well as imaging, were performed by Wuhan Pinuofei Biological Technology Company (China). The numbers of megakaryocytes and positively immunostained cells were determined using ImageJ software.

### 2.4 Cell purification and cultivation

We purified splenic naive CD4<sup>+</sup> T cells from 8-week-old female C57BL/6 WT mice using the MojoSort™ CD4<sup>+</sup> Naive T Cell Isolation Kit (480041,

BioLegend, San Diego, CA, USA). In the expansion and activation assays,  $1 \times 10^5$  cells were placed in 96-well plates with 200  $\mu$ L of medium per well and stimulated with the T Cell Activation and Expansion Kit (130-093-627, Miltenyi Biotec, Bergisch Gladbach, Germany). Dry powders of the OX40L recombinant protein (CM74, novoprotein, Beijing, China) were dissolved in sterilized deionized water. The cell samples were harvested and stimulated with or without 4 mg/mL OX40L recombinant protein (CM74, novoprotein). After culture for 6 d, the culture supernatants and cell samples were subjected to enzyme-linked immunosorbent assay (ELISA) and flow cytometry (FCM) analysis, respectively.

## 2.5 ELISA

The levels of IL-4, IL-6, IL-10, IL-17A, IL-21, and transforming growth factor- $\beta$  (TGF- $\beta$ ) in the serum or culture supernatants were measured via ELISA kits (Proteintech, China). The experiments were performed in accordance with the manufacturer's protocols. The absorbance of samples was measured with a Synergy Neo2 multimode reader (BioTek, Vermont, USA) at 450 nm, and the serum concentrations of cytokines were calculated using standard curves.

## 2.6 Western blotting

Total proteins were extracted from the control and ITP model mice with a total protein extraction kit (BestBio, Shanghai, China). The albumin concentration of spleen samples was quantified by a bicinchoninic acid (BCA) assay kit (BestBio). The proteins were separated via 10% (0.1 g/mL) sodium dodecyl sulfate-polyacrylamide gel electrophoresis (SDS-PAGE) at 80 V. Subsequently, the proteins were transferred to polyvinylidene fluoride membranes (Millipore, Billerica, MA, USA) at 330 mA for 60 min and blocked with 0.05 g/mL skimmed milk (Solarbio, Beijing, China). The protein membranes were incubated with primary antibodies (Abs) overnight at 4 °C and then with the appropriate secondary horseradish peroxidase (HRP)-conjugated Abs for 1 h. Images of the protein bands were ultimately taken with the ChemiDoc MP imaging system (Bio-Rad, Hercules, CA, USA). Protein gray-scale analysis was conducted with ImageJ software.

## 2.7 FCM analysis

Before staining, the cells were incubated with Fc-blocking antibody for 15 min, subsequently washed

with stain buffer (fetal bovine serum (FBS), BD Biosciences, San Jose, CA, USA) and centrifuged at 300g for 5 min. The fixable viability stain 440UV (BD Biosciences) was then used to stain dead cells for 15 min. The samples were washed with stain buffer and centrifuged at 300g for 5 min. Subsequently, the cells were preincubated with brilliant stain buffer (BD Biosciences) for 15 min. The cell samples were then stained with APC-Cy7-conjugated anti-mouse CD3, BUV496-conjugated anti-mouse CD4, fluorescein isothiocyanate (FITC)-conjugated anti-mouse CD8, BB700-conjugated anti-mouse CD45RA, BV421-conjugated anti-mouse CXCR5, BV605-conjugated anti-mouse OX40, BV480-conjugated anti-mouse PD-1, and BV750-conjugated anti-mouse CD40 ligand (CD40L) (BD Biosciences), and with BV711-conjugated anti-mouse CD62L, BV785-conjugated anti-mouse C-C chemokine receptor type 6 (CCR6), and PE/Fire 810-conjugated anti-mouse CXCR3 (BioLegend) for 45 min. After surface staining, the samples were washed with stain buffer, centrifuged at 300g for 5 min, and resuspended in 200  $\mu$ L stain buffer. The data were obtained using the Sony ID7000 Spectral Cell Analyzer (Sony Biotechnology, Tokyo, Japan) and analyzed with FlowJo v10.8.1 software.

## 2.8 Statistical analysis

All data in our study were presented as mean  $\pm$  standard deviation (SD). The significance of differences between the control and ITP groups was determined using a *t*-test or Mann-Whitney *U*-test depending on the normality of the data. All statistical calculations were implemented using GraphPad Prism version 8.0 software, with a *P* value of <0.05 indicating statistical significance.

## 3 Results

### 3.1 Establishment of passive murine models of ITP (antibody injection)

In order to examine the vital role of OX40 in the immunopathological mechanisms of ITP, we established a passive ITP mouse model (Fig. 1a). First, an anti-mouse CD41 antibody was injected into the peritoneal cavity of C57BL/6 WT mice, and control mice were injected with the same volume of PBS. The mice treated with the monoclonal platelet antibody became thrombocytopenic; the platelet counts were significantly reduced within 24 h after injection and gradually decreased

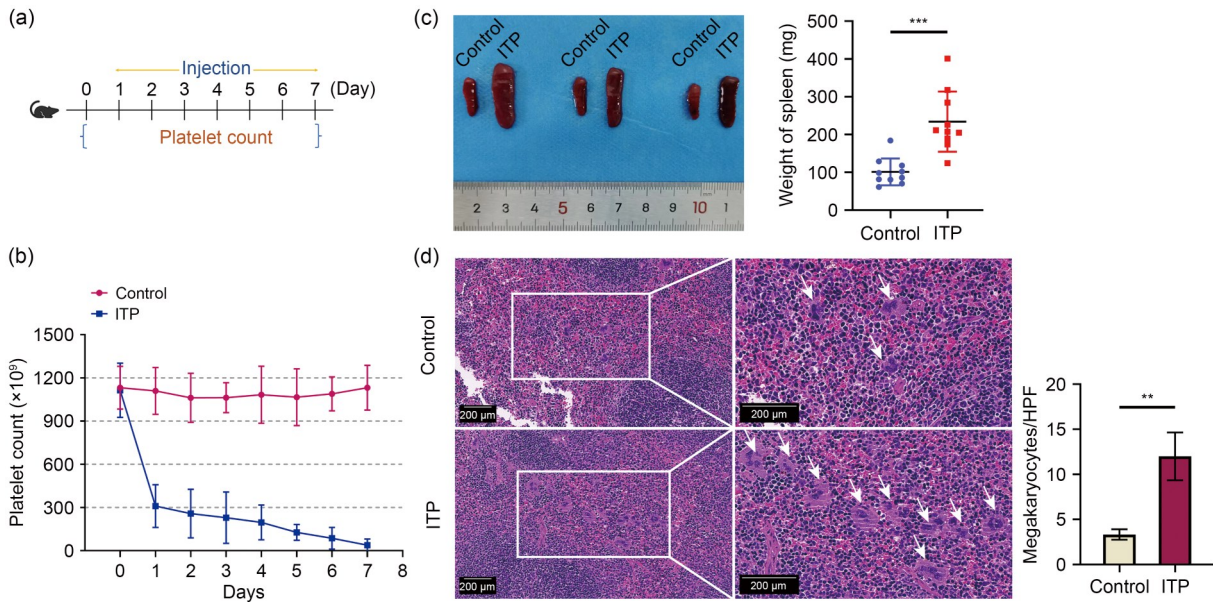


**Fig. 1** Assessment of platelet count, splenomegaly, and megakaryocytes in the spleen. (a) Flowchart of the passive immune thrombocytopenia (ITP) murine model. (b) Peripheral blood was extracted at different time points for measuring platelet count ( $n=10$ ). (c) Wet weights of spleens and gross appearance of representative spleen tissues in control and ITP mice ( $n=10$ ). (d) Photomicrograph of hematoxylin and eosin (H&E) staining of pathological changes of the spleens in ITP mice ( $n=3$ ). HPF: high-power field. Data are expressed as mean±standard deviation (SD). Significant differences are indicated by  $**P<0.01$  and  $***P<0.001$ .

from Day 2 to Day 7 (Fig. 1b). Meanwhile, platelet counts in the control mice remained stable throughout the study (Fig. 1b). Compared to those of the controls, the spleens of the ITP model mice exhibited abnormal appearance, with significantly greater enlargement and weight increase (Fig. 1c). In addition, histopathological examinations were performed on the spleens of the mice in the control and ITP groups. By H&E section observation, thrombocytopenic mice exhibited significant histopathological changes compared to control mice. In the spleens of mice with ITP, the lymphocytes were dense and the red blood sinuses were expanded (Fig. 1d). Compared to those in the controls, a greater percentage of infiltrating megakaryocytes in the spleen was observed in the model group (Fig. 1d). In addition, the antiplatelet agent MWReg30 induced morphological aberrations of megakaryocytes, which consisted of pyknotic nuclei and cytoplasmic blebbing (Fig. 1d).

### 3.2 Abnormal expression levels of OX40L–OX40 in ITP model mice

The costimulatory signals of OX40L–OX40 play a major role in the pathophysiology of autoimmune diseases (Edner et al., 2020). To explore the potential

roles of OX40L and OX40 in aggravating the pathogenesis of ITP, the protein levels of OX40L and OX40 in the spleens of control and ITP model mice were determined via western blotting and IHC assays. For both datasets, the results showed that the expression levels and positive immunostaining of splenic OX40L and OX40 in ITP model mice were markedly higher than those in normal controls (Figs. 2a and 2b). Interestingly, OX40-positivity was detected in the germinal center (GC) of the white pulp in the splenic lymphoid nodule of ITP model mice (Fig. 2b).

### 3.3 Effect of OX40L–OX40 immunoregulatory axis on Tfh differentiation in vitro

Antiplatelet antibody-producing B lymphocytes play a critical role in the pathogenesis of ITP (Audia et al., 2021). In the GC, the maturation of high-affinity B-cell clones depends on support from Tfh cells (Liu et al., 2021). The costimulating signal of the OX40L–OX40 axis is important for T-cell activation and function. To evaluate the potential effects of OX40L and OX40 on Tfh cells, we purified splenic CD4<sup>+</sup> naive T cells from C57BL/6 WT mice via activation with anti-CD3e/CD28 beads with or without incubation with the recombinant protein OX40L for 6 d. The phenotype

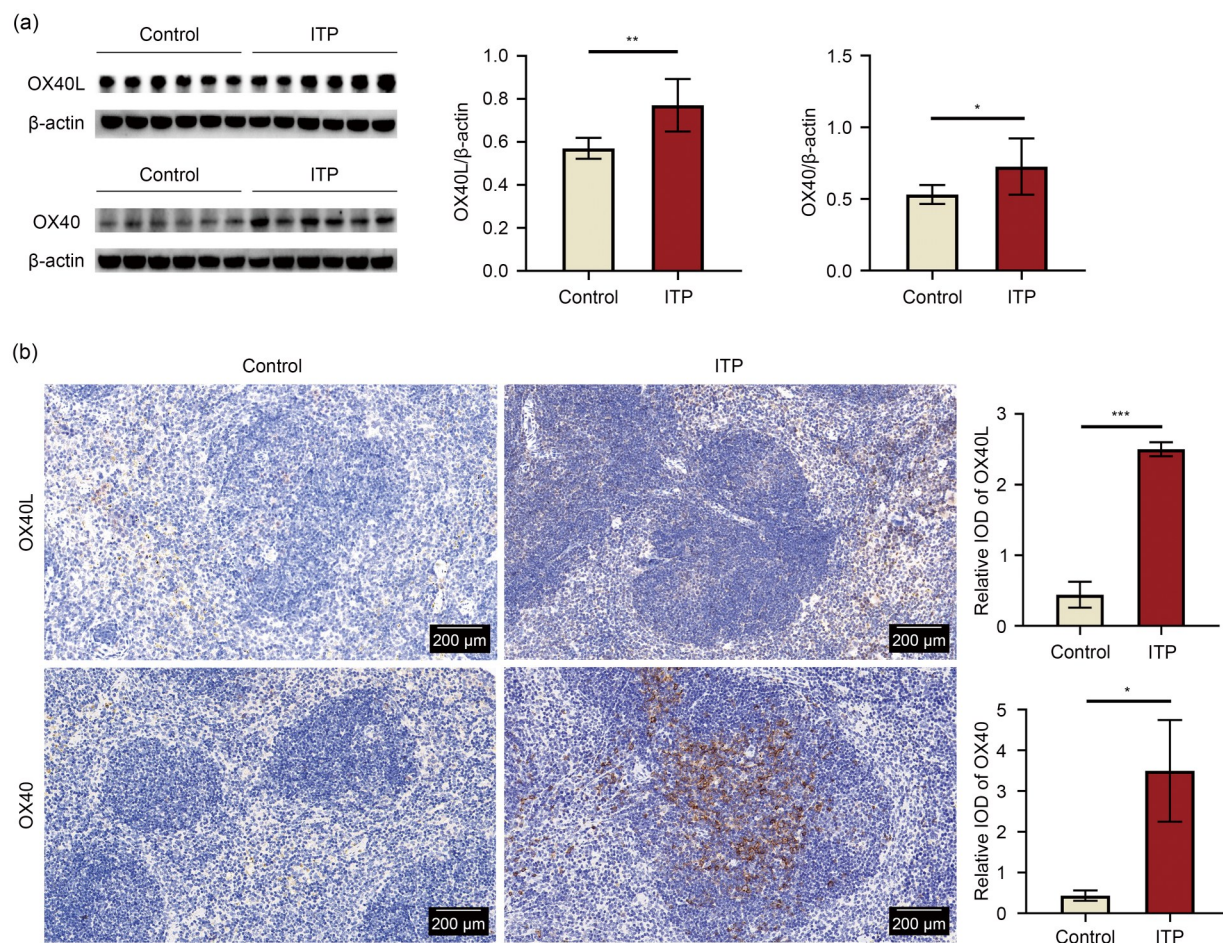


**Fig. 2** Upregulated expression of OX40 ligand (OX40L) and OX40 in the spleens of immune thrombocytopenia (ITP) mice. (a) The protein levels of OX40L and OX40 in the spleens of ITP mice ( $n=6$ ). (b) Immunohistochemical (IHC) staining for OX40L and OX40 performed on splenic tissues ( $n=3$ ). IOD: integrated optical density. Data are expressed as mean $\pm$ standard deviation (SD). Significant differences are indicated by \* $P<0.05$ , \*\* $P<0.01$ , and \*\*\* $P<0.001$ .

and expression of specific markers OX40, ICOS, PD-1, and CD40L in Tfh cells were examined by FCM.

Compared to those in the controls, the frequencies of  $CD4^+CD45RA^-CXCR5^+$  Tfh cells in the group treated with OX40L were significantly greater after 6 d of differentiation and the expression of ICOS, PD-1, and CD40L was upregulated (Figs. 3a and 3c–3e). Meanwhile, the expression of OX40 in Tfh cells were significantly downregulated in the OX40L-stimulated group, indicating that OX40L increased binding to OX40 (Fig. 3b). Next, we examined the levels of several Tfh-related cytokines in the cell supernatant. In the OX40L-treated group, the concentrations of IL-4, IL-17A, and IL-21 were significantly increased (Fig. 3f). These data indicated that the surface-bound molecule OX40L combined with OX40 promotes Tfh cell differentiation and function in vitro (Fig. 3a).

### 3.4 Function of OX40L–OX40-mediated Tfh differentiation in ITP model mice

In order to further study the differentiation and function of Tfh cells in the ITP model mice, we measured the phenotype of splenic T cells and the expression levels of characteristic markers in Tfh cells in the control and ITP model mice. In the ITP group, the Tfh molecules CXCR5, Bcl6, ICOS, PD-1, and CD40L were upregulated (Fig. 4a). Splenic Tfh cells were also analyzed by FCM in the present study, and we observed a 1.3-fold increase in the percentage of  $CD4^+CD45RA^-CXCR5^+$  Tfh cells in ITP model mice compared to that in controls (Fig. 4b). According to the documented gating strategy, we further investigated three Tfh cell subtypes, Tfh1 ( $CXCR3^+CCR6^-$ ), Tfh2 ( $CXCR3^-CCR6^-$ ), and Tfh17 ( $CXCR3^-CCR6^+$ ) cells in the spleens of

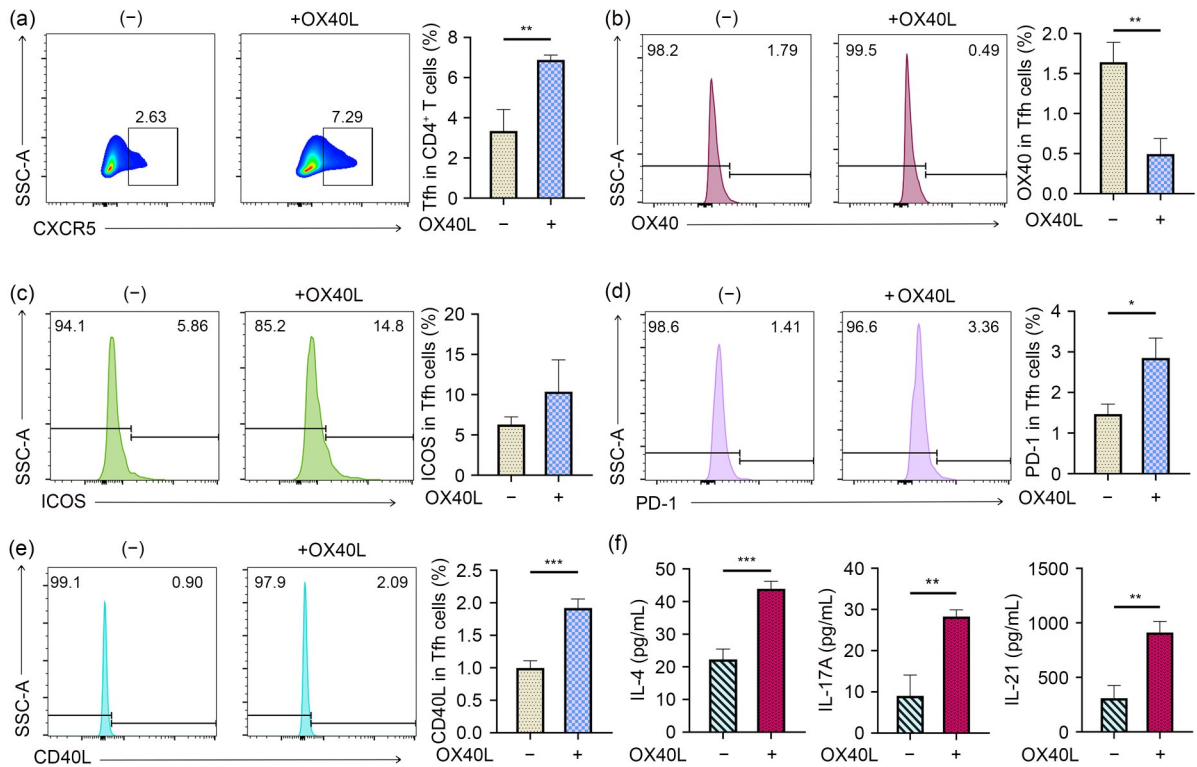


**Fig. 3** Effects of OX40 ligand (OX40L)–OX40 axis on follicular helper T (Tfh) differentiation and development in vitro. Purified splenic cluster of differentiation 4-positive (CD4<sup>+</sup>) naive T cells were activated by anti-CD3e/CD28 beads and cultured in the presence or absence of recombinant protein OX40L for 6 d. (a) Frequency of Tfh cells among the total CD4<sup>+</sup> T cells from normal and ITP mice. CXCR5: CXC chemokine receptor type 5; SSC-A: side scatter-area. (b) Percentage of OX40 expression on Tfh cells. (c) Percentage of inducible T-cell costimulator (ICOS) expression on Tfh cells. (d) Percentage of programmed cell death protein-1 (PD-1) expression on Tfh cells. (e) Percentage of CD40 ligand (CD40L) expression on Tfh cells. (f) Levels of interleukin (IL)-4, IL-17A, and IL-21 in the culture supernatants. Data are expressed as mean ± standard deviation (SD), *n*=3. Significant differences are indicated by \**P*<0.05, \*\**P*<0.01, and \*\*\**P*<0.001.

control and ITP model mice (Bonami et al., 2020). Compared to the controls, the percentage of Tfh2 cells was greater, but the percentage of Tfh1 cells was lower in the ITP model mice (Fig. 4b). The percentage of Tfh17 cells was extremely low, with no significant difference between the two groups (Fig. 4b). The Tfh1/Tfh2 cell ratio in ITP model mice was lower than that in normal mice (Fig. 4b). These findings imply that the cell populations exhibited a Tfh1-to-Tfh2 shift in mice with ITP. Furthermore, the expression of the key Tfh activation markers OX40, ICOS, and PD-1 on Tfh2 cells was significantly increased in ITP model mice, while that of CD40L slightly increased, with no statistical significance (Fig. 4c). We further assessed the plasma levels of pro- and anti-inflammatory cytokines that are related to Tfh differentiation and ITP pathogenesis. As shown in Fig. 4d, in the serum of ITP model mice, the secretion of the proinflammatory cytokines IL-4, IL-6, IL-17A, and IL-21 was increased, whereas the secretion of the

anti-inflammatory cytokines IL-10 and TGF-β was decreased. These data imply that OX40L–OX40 coupling might stimulate the proliferation, expansion, and function of Tfh cells and shift Tfh populations to Tfh2 cells in ITP.

### 3.5 Colocalization of OX40 with Tfh and B cells during the migration of B cells to germinal centers in ITP model mice

In order to determine the localization of OX40, we stained spleen tissues from control and ITP model mice with anti-CD4, anti-CXCR5, anti-CD19, and anti-OX40 antibodies. In the spleens of ITP model mice, OX40 was highly expressed in the GCs of the white pulp and colocalized with CD4 and CXCR5 (Figs. 5a and 5b). These results suggest that OX40L–OX40 coupling might contribute to aberrant Tfh cell activation in ITP. Splenic CD4<sup>+</sup>CD19<sup>+</sup> B cells from normal mice were found mainly in the marginal zone, whereas CD4<sup>+</sup>CD19<sup>+</sup>

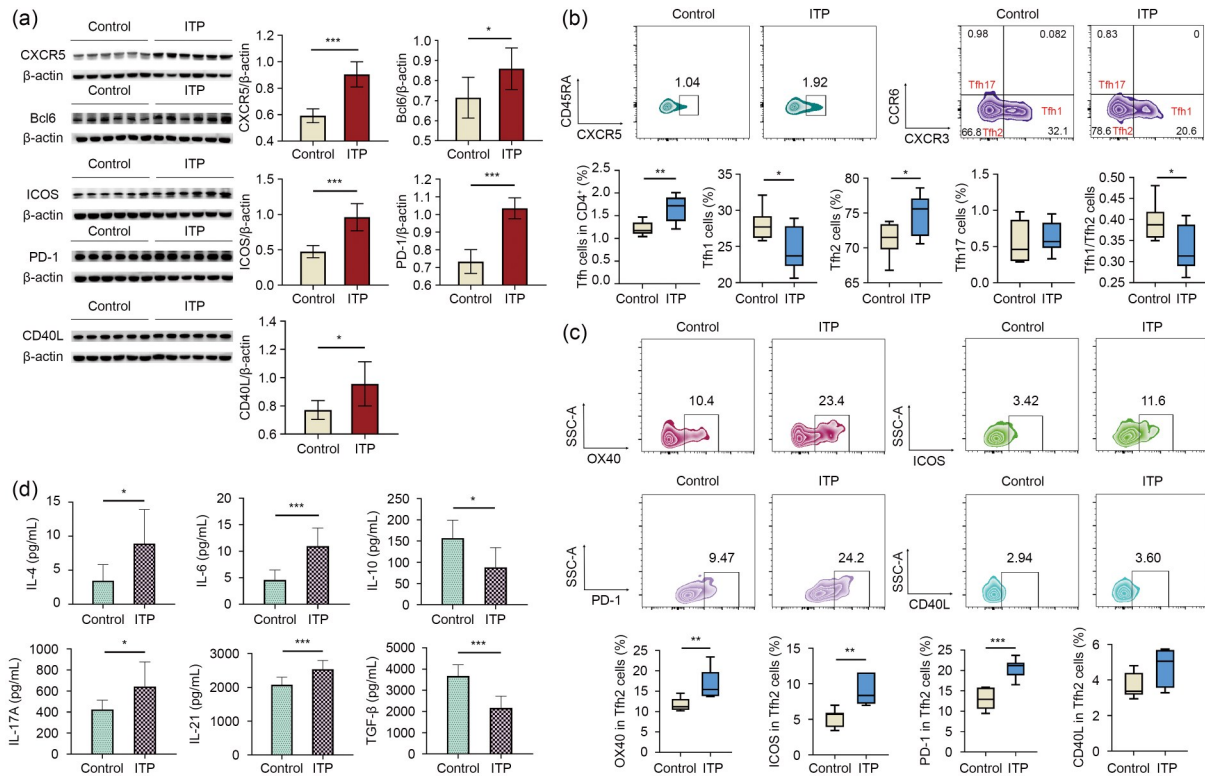


**Fig. 4** Differentiation and function of follicular helper T (Tfh) subtypes in immune thrombocytopenia (ITP) mice. (a) Expression of key molecules (CXC chemokine receptor type 5 (CXCR5), B-cell lymphoma 6 (Bcl6), inducible T-cell costimulator (ICOS), programmed cell death protein-1 (PD-1), and cluster of differentiation 40 ligand (CD40L)) of Tfh cells in the spleens of normal and ITP mice ( $n=6$ ). (b) Frequencies of splenic CXCR5<sup>+</sup>CD45RA<sup>-</sup> Tfh cells and Tfh subtypes in normal and ITP mice ( $n=7$ ); CXCR3<sup>+</sup>CCR6<sup>-</sup> represents Tfh1, CXCR3<sup>-</sup>CCR6<sup>-</sup> represents Tfh2, and CXCR3<sup>-</sup>CCR6<sup>+</sup> represents Tfh17. (c) Expression of OX40, ICOS, PD-1, and CD40L on Tfh2 cells ( $n=7$ ). (d) Levels of proinflammatory cytokines (interleukin (IL)-4, IL-6, IL-17A, and IL-21) and anti-inflammatory cytokines (IL-10 and transforming growth factor- $\beta$  (TGF- $\beta$ )) in the serum of normal and ITP mice ( $n=10$ ). SSC-A: side scatter-area. Data are expressed as mean  $\pm$  standard deviation (SD). Significant differences are indicated by \* $P<0.05$ , \*\* $P<0.01$ , and \*\*\* $P<0.001$ .

B cells from the spleens of ITP model mice were abundantly distributed in the GCs of white pulp and colocalized with CD4, CXCR5, and OX40 (Fig. 5b). Taken the above findings together, we speculated that the aberrant expression of OX40L and OX40 increases Tfh cell differentiation and helper function. Subsequently, Tfh cells may interact with B lymphocytes, which promotes their migration to GCs and their maturation into antibody-produced plasma cells. The OX40L–OX40 axis plays a pivotal role in ITP pathogenesis; however, the specific regulatory mechanism of Tfh cells' helper function on B lymphocytes in ITP, regulated by this axis, needs to be further explored.

### 3.6 Signaling pathways associated with Tfh differentiation in ITP model mice

We confirmed that the OX40L–OX40 axis plays an essential role in Tfh cell differentiation and development

in ITP, but the downstream signaling pathways of OX40L–OX40 in Tfh-mediated ITP remained to be discovered. Previously, the signaling mechanism of OX40 was considered to be associated with the activation of the TRAF–NF- $\kappa$ B pathway (Pedros et al., 2018). To assess the possible regulatory mechanisms of the OX40L–OX40 axis in ITP, we extended our study by investigating the expression of TRAF proteins and the activation of NF- $\kappa$ B pathway in an ITP mouse model. Among the six members of the TRAF protein family (TRAF1–6), TRAF2, TRAF3, TRAF4, and TRAF5 were significantly upregulated in the ITP mouse model (Fig. 6a). The protein level of TRAF1 or TRAF6 was not significantly different between the control and ITP groups (Fig. 6a). Moreover, the NF- $\kappa$ B pathway was activated in ITP model mice, as evidenced by a significantly increased ratio of phospho-p65 (p-p65)/p65 (Fig. 6a). Crosstalk between the JAK–STAT pathway

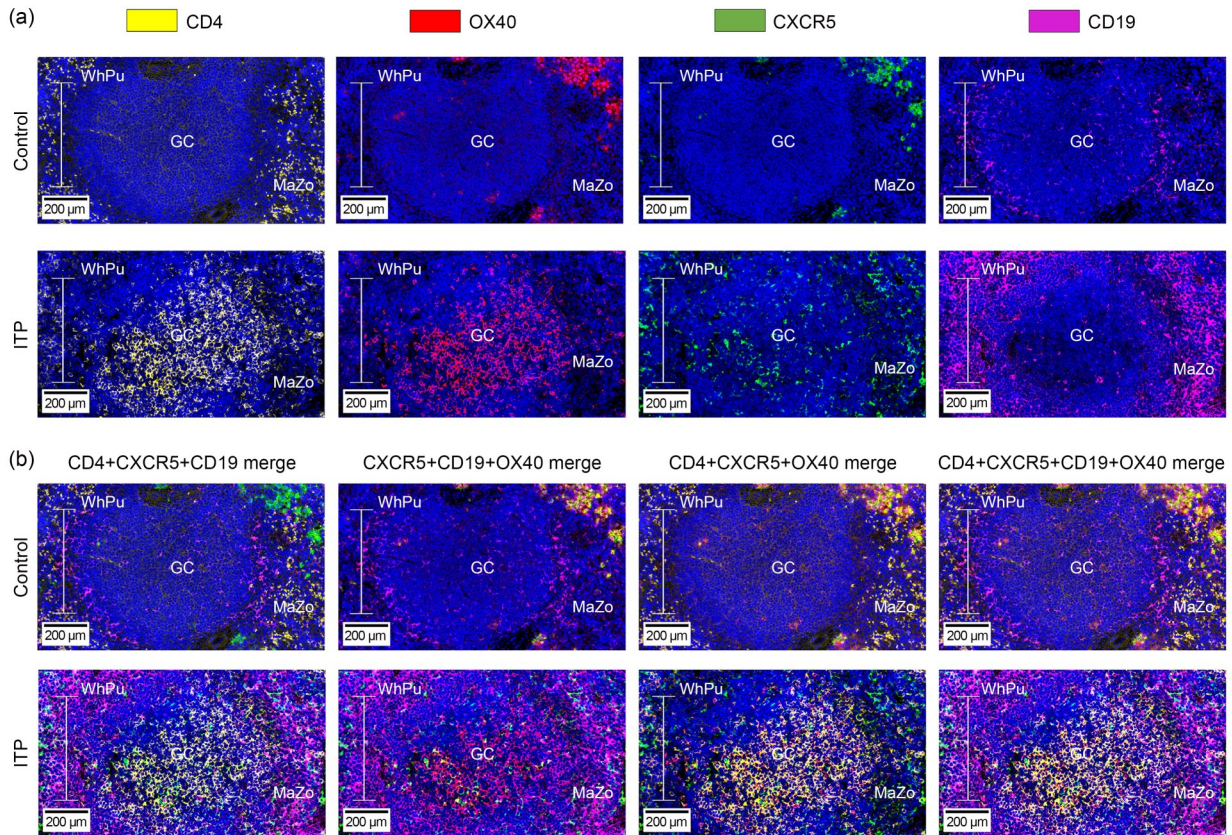


**Fig. 5** Expression and localization of OX40, follicular helper T (Tfh) cells, and B cells in the spleens of normal and immune thrombocytopenia (ITP) mice. (a) Individual markers cluster of differentiation 4 (CD4), OX40, CXC chemokine receptor type 5 (CXCR5), and CD19 of images. (b) Composite images of multiple markers. WhPu, GC, and MaZo represent white pulp, germinal center, and marginal zone, respectively.

and TRAF-mediated pathway has been reported in previous research (Nagashima et al., 2018). Therefore, to assess the activation of the JAK–STAT pathway, we further evaluated the expression and phosphorylation of JAK kinases and STAT family members in ITP model mice. Compared to that in normal mice, the p-JAK3/JAK3 ratio was significantly lower, whereas the phosphotyrosine kinase 2 (p-Tyk2)/Tyk2 ratio was notably greater in ITP model mice (Fig. 6b). The p-JAK1/JAK1 or p-JAK2/JAK2 ratio was not significantly different between the two groups (Fig. 6b). In the ITP mouse model, western blotting analysis demonstrated a notable increase in the p-STAT3/STAT3 and p-STAT6/STAT6 ratios and a significant decrease in the p-STAT2/STAT2 and p-STAT5/STAT5 ratios (Fig. 6c). Taken together, the above data suggest that OX40 might activate the downstream TRAF–NF- $\kappa$ B signaling pathway and cross-talk with the JAK–STAT pathway, regulating Tfh differentiation in ITP model mice.

## 4 Discussion

ITP is a complicated autoimmune disease characterized by impaired platelet generation and exacerbated platelet injury (Mingot-Castellano et al., 2022). Some ITP patients with prolonged and severe thrombocytopenia are insensitive to current therapies, and these patients also have an increased risk of bleeding and complications (Vianelli et al., 2022; Cines, 2023). Therefore, the identification of novel therapeutic methods for ITP is necessary.

The OX40L–OX40 axis has been proposed as a promising target for treating autoimmunity (Furie and Furie, 2021). A previous study indicated the crucial role of the OX40L–OX40 interaction in the immunopathological mechanisms of autoimmune diseases, such as SLE, RA, and allergic asthma (Cui et al., 2019). In an SLE mouse model, the expression of OX40 on several CD4<sup>+</sup> T-cell subsets was enhanced in kidney and spleen

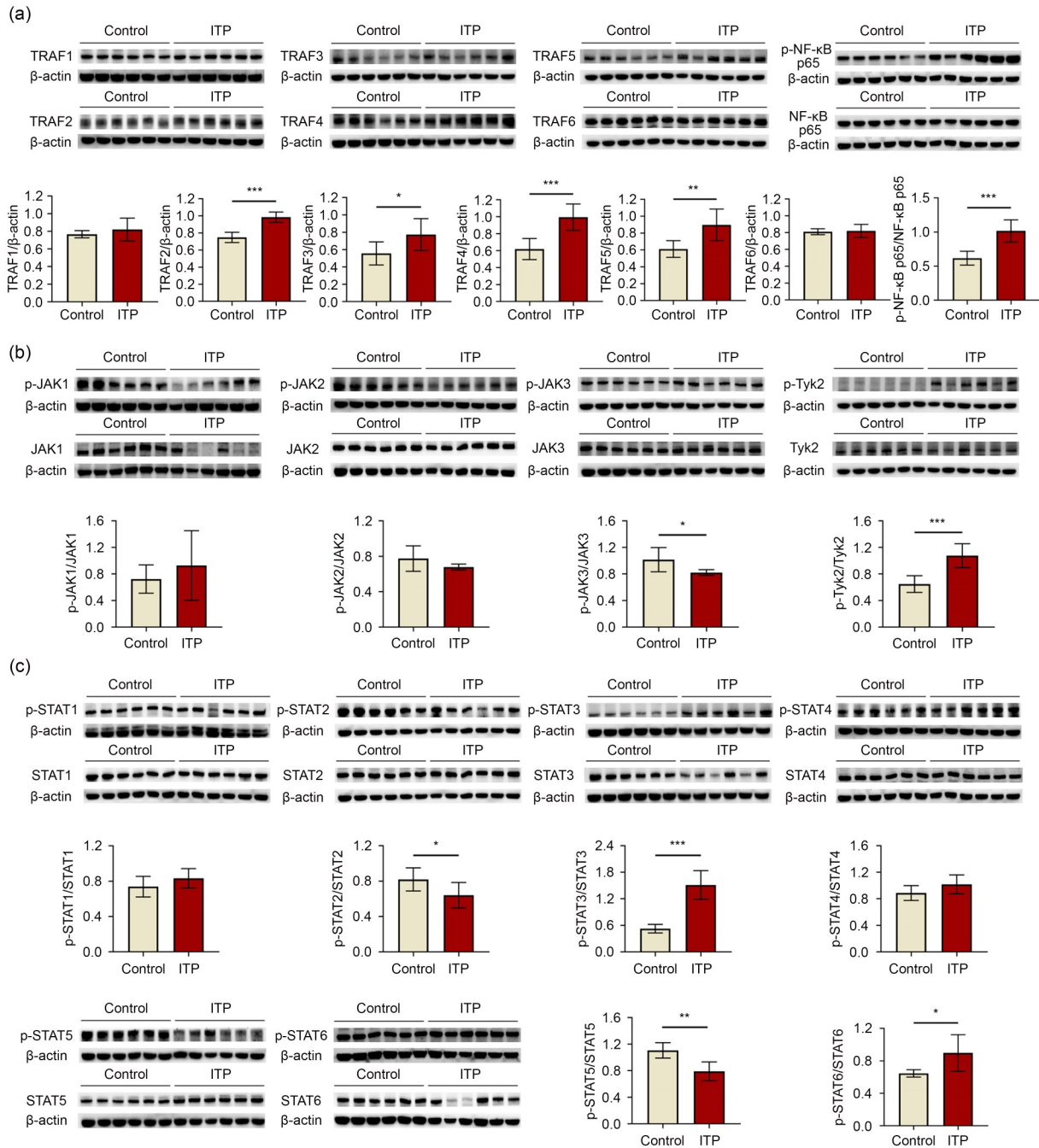


**Fig. 6** Activation of tumor necrosis factor receptor-associated factor (TRAF)–nuclear factor-κB (NF-κB) and Janus kinase (JAK)–signal transducer and activator of transcription (STAT) signal pathways in normal and immune thrombocytopenia (ITP) mice. (a) Expression of TRAF proteins and phosphorylation of NF-κB p65 in the spleens of normal and ITP mice. (b) Phosphorylation of JAKs in the spleens of normal and ITP mice. (c) Phosphorylation of STATs in the spleens of normal and ITP mice. Data are expressed as mean±standard deviation (SD), *n*=6. Significant differences are indicated by \**P*<0.05, \*\**P*<0.01, and \*\*\**P*<0.001.

tissues and this was correlated with disease severity (Sitrin et al., 2017). OX40L expression tended to increase in RA patients, and it also increased in an age-dependent manner in the serum of healthy volunteers

(An et al., 2019). In our previous study, to explore the clinical significance of *OX40L* and *OX40* expression in ITP patients, we collected samples from 54 newly diagnosed ITP patients and 24 healthy controls (HCs).

Compared with HCs, the expression levels of *OX40L* and *OX40* mRNA in PBMCs were significantly up-regulated in ITP patients, accompanied by significantly elevated  $OX40^+CD4^+$  T cells' frequencies and plasma soluble *OX40L* (s*OX40L*) levels (Cui et al., 2019). In the present study, we discovered that splenic *OX40L* and *OX40* were significantly upregulated in mice with ITP, similar to the findings of previous research (Cui et al., 2019). On this basis, we inferred that the abnormal expression of *OX40L* and *OX40* might contribute to the development of ITP. Numerous studies have shown that the costimulatory signals of *OX40L*–*OX40* can support Tfh cell development and survival and enhance the ability of Tfh cells to support B lymphocytes (Fu et al., 2021). Jacquemin et al. (2015) discovered that *OX40L* and *OX40* are involved in the abnormal Tfh response in patients with SLE (Jacquemin et al., 2015). Recently, many studies have shown that abnormal *OX40L* and *OX40* expression on regulatory T cells (Tregs) and follicular regulatory T (Tfr) cells impairs the ability of Tfh cell-dependent B lymphocyte activation (Jacquemin et al., 2018). In our survey, we found that *OX40L* increased the expression of multiple Tfh cell molecules (ICOS, PD-1, and CD40L) and promoted effector cytokine secretion (IL-4, IL-17A, and IL-21), likely enhancing the helper function of Tfh cells for B cells in vitro. Consistent with the in vivo results, in the ITP mouse model, the percentage of  $OX40^+$  Tfh cells increased, and this change was accompanied by the high expression of characteristic molecules strongly related to Tfh cell differentiation and function. These data implied that upregulated *OX40*-mediated abnormal Tfh activity might play a major pathogenic role in ITP.

In order to explore the interaction between *OX40L*–*OX40*, Tfh cells, and B cells in ITP, we conducted immunofluorescence staining of spleen tissues from control and ITP model mice. The immunofluorescence images showed that splenic  $CD4^+CD19^+$  B cells in ITP model mice were concentrated in the GC of the white pulp and colocalized with Tfh cells and *OX40*, while  $CD4^+CD19^+$  B cells in normal mice were distributed in the marginal zone. *OX40L*–*OX40* costimulatory signals play critical roles in improving the function of T cells, enhancing their survival, and preventing their apoptosis (Fu et al., 2021). Jacquemin et al. (2018) discovered that *OX40L*–*OX40* could induce the expression of multiple molecules on human-derived Tfh

cells and promote them to become functional B cell helpers in vitro (Jacquemin et al., 2018). A previous study considered that *OX40L*–*OX40* interaction could promote both GC Tfh and GC B cell differentiation, and accelerate B cell differentiation into plasma cells with the help of GC Tfh cells (Fu et al., 2021). Antiplatelet autoantibodies produced by B lymphocytes are the main pathogenic factors for ITP; they not only increase platelet destruction but also impair the ability of megakaryocytes to generate platelets (Wang et al., 2020). The majority of antiplatelet antibodies are specifically generated by long-lived plasma cells in the spleen and the bone marrow (Vernava and Schmitt, 2023). In the resting state, B lymphocytes are mainly located in the T-cell zone and the marginal zone in the spleen (Victoria and Nussenzweig, 2022). After antigen stimulation, B cells are activated and migrate to GCs, where Tfh cells help B lymphocytes differentiate into long-lived plasma cells to produce antiplatelet antibodies against glycoproteins (like GPIIb/IIIa and GPIb/IX) in thrombocytes and megakaryocytes (Victoria and Nussenzweig, 2022; Vernava and Schmitt, 2023). Antiplatelet antibodies can target glycoproteins, especially the GPIIb/IIIa, through interactions with Fc gamma receptors (FcγRs) and complement receptors, inducing platelet phagocytosis (Audia et al., 2021). Indeed, a study reported that splenic Tfh cells were increased and this was correlated with increased GCs and plasma cells in ITP patients (Audia et al., 2014). In vitro, the activation of Tfh cells promoted the differentiation of splenic B cells into plasma cells and induced the secretion of antiplatelet antibodies in ITP patients (Audia et al., 2014). These data suggested that up-regulated *OX40* signaling might induce abnormal Tfh activity, promoting the establishment of GCs and regulating the migration, differentiation, and maturation of antibody-secreting B lymphocytes. Overall, *OX40* signaling likely contributes to the production of autoantibodies by enhancing the helper function of Tfh cells for B lymphocytes, resulting in the acceleration of ITP progression.

Because of the important effect of Tfh cells on ITP pathogenesis, our study further explored the subtype distribution of Tfh cells in an ITP animal model. The results indicated that the percentages of Tfh1 and Tfh2 cells in the spleens of ITP model mice decreased and increased, respectively, and the ratio of Tfh1/Tfh2 cells decreased. The percentage of Tfh17 cells was extremely

low in the present study, so further analysis of this subset was not performed. Similar trends have been observed in other autoimmune diseases in other studies. For instance, Xu et al. (2019) reported that antineutrophil cytoplasmic antibody (ANCA)-associated vasculitis (AAV) patients exhibit a Tfh1-to-Tfh2 shift, with a decrease in Tfh1 cells and an increase in Tfh2 cells. Moreover, in ankylosing spondylitis (AS) patients, a high degree of disease activity was associated with elevated Tfh2 effector memory levels (Shesternya et al., 2022). Patients with juvenile dermatomyositis also had an increased ratio of Tfh2/Tfh1 cells, with Tfh1 cells incapable of assisting naive B lymphocytes (Morita et al., 2011; Schmitt et al., 2014). These findings illustrated that changes in the subtype composition of Tfh cells (Tfh1-to-Tfh2 shift) might participate in the progression of ITP and that Tfh2 cells likely play a major role in promoting B lymphocyte differentiation and development.

To further verify the molecular mechanisms of OX40L–OX40 signaling in ITP, the downstream interacting proteins and phosphorylation pathways of OX40 were explored, and the expression of TRAF2, TRAF3, TRAF4, and TRAF5 was significantly increased in the ITP mouse model. OX40 is a TRAF-dependent TNF receptor superfamily (TNFRSF) member associated with the differentiation and function of Tfh cells (Pedros et al., 2018). OX40L binding to OX40 results in the recruitment of TRAF2, TRAF3, and TRAF5 (Fu et al., 2021). Previous studies have reported that OX40 ligation by OX40L can promote the assembly of a unique complex TRAF–receptor-interacting protein (RIP)–inhibitor of  $\kappa$ B kinase  $\alpha/\beta/\gamma$  (IKK $\alpha/\beta/\gamma$ ) that activates NF- $\kappa$ B to provide survival signals to T cells (So et al., 2011). NF- $\kappa$ B activation plays an essential role in T-cell responses, and TRAFs are viewed as strong activators of NF- $\kappa$ B for T-cell immunity (So et al., 2011). Researchers discovered that activated OX40 signaling proteins can interact with TRAF2 and TRAF5, promoting the NF- $\kappa$ B pathway to positively regulate Tfh differentiation (Nagashima et al., 2018; Furue and Furue, 2021). Moreover, TRAF3 plays an important role in the conduction of OX40 signaling and may also inhibit OX40 activation and Tfh development (Nagashima et al., 2018). TRAF6 could induce the activation of the non-canonical NF- $\kappa$ B pathway in the presence of OX40 ligation (Xiao et al., 2012). Aberrant ubiquitination of TRAF6 can also facilitate the activation of the NF- $\kappa$ B pathway; however, TRAF6 levels were not significantly different between the control and ITP groups in our study

(Yang et al., 2023). He et al. (2018) suggested that NF- $\kappa$ B expression significantly increases in ITP patients, and overexpressed NF- $\kappa$ B co-incubation with CD34<sup>+</sup> cells can result in a reduction in megakaryocytic differentiation and thrombopoiesis in vitro, indicating the important role of the NF- $\kappa$ B signal in ITP pathogenesis. Certainly, we observed increased phosphorylation of the NF- $\kappa$ B p65 protein in the spleens of ITP model mice. Nonetheless, more experiments should be conducted to further clarify the role of OX40L–OX40 axis in mediating TRAF–NF- $\kappa$ B to regulate ITP pathogenesis. Additionally, the JAK–STAT pathway, which is generated by the cytokine receptors IL-6 and IL-21, influences Tfh cell development, and its interactions with TRAF-mediated pathways can facilitate the generation of the integrated signals required to induce and maintain Tfh differentiation (Nagashima et al., 2018). In this study, the levels of IL-6 and IL-21 in the serum of ITP model mice were increased. The p-Tyk2/Tyk2, p-STAT3/STAT3, and p-STAT6/STAT6 ratios were notably raised, while the p-JAK3/JAK3, p-STAT2/STAT2, and p-STAT5/STAT5 ratios were significantly decreased. Thus, we speculated that the OX40–OX40 axis might activate the TRAF–NF- $\kappa$ B pathway in ITP, promoting Tfh differentiation. Subsequently, the secretion of the Tfh-related cytokines IL-6 and IL-21 was increased, which acted on cytokine receptors of Tfh cells, inducing the activation of the JAK–STAT signaling pathway, promoting Tfh differentiation. However, the regulatory mechanism of the OX40L–OX40 downstream signaling pathway in ITP is complex and needs further exploration by experiments.

In the present work, we constructed a passive ITP mouse model of MWReg30. Compared to the controls, MWReg30 induced a significant reduction in the platelet counts of ITP model mice, leading to spleens exhibiting enlargement, weight increase, and aberrant histopathological changes. MWReg30 was discovered by Burstein et al. (1992) and has been widely used to construct passive ITP animal models (Burstein et al., 1992; Guo et al., 2018). Guo et al. (2018) found that MWReg30 could reduce the platelet counts and significantly increase the number of bone marrow megakaryocyte counts. Similarly, we observed a higher concentration infiltration of megakaryocytes in the spleen of ITP model mice. Yu et al. (2018) used the passive ITP mouse model to validate the progranulin deficiency impairing proliferation of Tregs. Li et al. (2019) established another efficient murine model of ITP through immunized CD41-KO

mice. Different from the ITP mouse model constructed with MWRReg30, the mature megakaryocytes in bone marrow were obviously decreased in this novel ITP murine model (Li et al., 2019). In the future, we aim to develop more efficient ITP murine models to make our conclusions more robust and explore the complicated pathophysiology of ITP.

## 5 Conclusions

Our study demonstrated that upregulated OX40L- and OX40-mediated abnormal Tfh activity plays a major pathogenic role in ITP. Aberrant OX40L–OX40 signaling might activate the TRAF–NF- $\kappa$ B and JAK–STAT signaling pathways. We speculated that the interactions between the two signaling pathways likely promote the Tfh1-to-Tfh2 shift, inducing the generation of autoantibodies by enhancing the helper function of Tfh cells for B cells, which results in the acceleration of the pathogenetic progression of ITP. Overall, our results suggest that the costimulation signaling pathway of OX40L–OX40 might be a potential therapeutic target for ITP. As a limitation of this study, we only used a passive ITP mouse model; therefore, additional investigations of the OX40L–OX40 axis mediating Tfh cell differentiation and function in ITP pathogenesis should be conducted in other efficient ITP murine models and clinical samples of ITP patients.

### Data availability statement

All data supporting the conclusions of the present study are included within this article.

### Acknowledgments

This work was supported by the National Natural Science Foundation of China (Nos. 82172335, 81971994, 91846103, and 81871709) and the Zhejiang Provincial Key Research and Development Program (No. 2020C03032), China.

We are grateful to Yidan ZHOU, Xiuyu WEI, and Yuan-yuan LV (from the Central Laboratory, The First Affiliated Hospital, Zhejiang University School of Medicine) for their help in using the Sony ID7000 Spectral Cell Analyzer.

### Author contributions

Ziyin YANG, Dawei CUI, and Jue XIE wrote the manuscript, and conceived and designed the study. Ziyin YANG and Lei HAI performed most of the experiments with help from Siwen WU and Yan LV. Ziyin YANG, Lei HAI, and Xiaoyu CHEN contributed to data analyses. All authors have read and

approved the final manuscript, and therefore, have full access to all the data in the study and take responsibility for the integrity and security of the data.

### Compliance with ethics guidelines

Ziyin YANG, Lei HAI, Xiaoyu CHEN, Siwen WU, Yan LV, Dawei CUI, and Jue XIE declare that they have no conflict of interest.

All the animal experiments were consented to by the Animal Ethics Committee of The First Affiliated Hospital, Zhejiang University School of Medicine, China (No. 2019621).

### References

- An JN, Ding SS, Hu XH, et al., 2019. Preparation, characterization and application of anti-human OX40 ligand (OX40L) monoclonal antibodies and establishment of a sandwich ELISA for autoimmune diseases detection. *Int Immunopharmacol*, 67:260-267. <https://doi.org/10.1016/j.intimp.2018.11.053>
- Audia S, Rossato M, Santegoets K, et al., 2014. Splenic TFH expansion participates in B-cell differentiation and antiplatelet-antibody production during immune thrombocytopenia. *Blood*, 124(18):2858-2866. <https://doi.org/10.1182/blood-2014-03-563445>
- Audia S, Mahévas M, Nivet M, et al., 2021. Immune thrombocytopenia: recent advances in pathogenesis and treatments. *Hemasphere*, 5(6):e574. <https://doi.org/10.1097/HS9.0000000000000574>
- Bonami RH, Nyhoff LE, McNitt DH, et al., 2020. T–B lymphocyte interactions promote type 1 diabetes independently of SLAM-associated protein. *J Immunol*, 205(12):3263-3276. <https://doi.org/10.4049/jimmunol.1900464>
- Burstein SA, Friese P, Downs T, et al., 1992. Characteristics of a novel rat anti-mouse platelet monoclonal antibody: application to studies of megakaryocytes. *Exp Hematol*, 20(10):1170-1177.
- Caza T, Wijewardena C, Al-Rabadi L, et al., 2022. Cell type-specific mechanistic target of rapamycin-dependent distortion of autophagy pathways in lupus nephritis. *Transl Res*, 245:55-81. <https://doi.org/10.1016/j.trsl.2022.03.004>
- Chen YW, Luo LP, Zheng YZ, et al., 2022. Association of platelet desialylation and circulating follicular helper T cells in patients with thrombocytopenia. *Front Immunol*, 13:810620. <https://doi.org/10.3389/fimmu.2022.810620>
- Cines DB, 2023. Pathogenesis of refractory ITP: overview. *Br J Haematol*, 203(1):10-16. <https://doi.org/10.1111/bjh.19083>
- Cui DW, Lv Y, Yuan XW, et al., 2019. Increased expressions of OX40 and OX40 ligand in patients with primary immune thrombocytopenia. *J Immunol Res*, 2019:6804806. <https://doi.org/10.1155/2019/6804806>
- Edner NM, Carlesso G, Rush JS, et al., 2020. Targeting costimulatory molecules in autoimmune disease. *Nat Rev Drug Discov*, 19(12):860-883.

- <https://doi.org/10.1038/s41573-020-0081-9>  
Fu NN, Xie F, Sun ZW, et al., 2021. The OX40/OX40L axis regulates T follicular helper cell differentiation: implications for autoimmune diseases. *Front Immunol*, 12:670637. <https://doi.org/10.3389/fimmu.2021.670637>
- Fu Y, Lin Q, Zhang ZR, et al., 2020. Therapeutic strategies for the costimulatory molecule OX40 in T-cell-mediated immunity. *Acta Pharm Sin B*, 10(3):414-433. <https://doi.org/10.1016/j.apsb.2019.08.010>
- Furue M, Furue M, 2021. OX40L–OX40 signaling in atopic dermatitis. *J Clin Med*, 10(12):2578. <https://doi.org/10.3390/jcm10122578>
- Ghanima W, Gernsheimer T, Kuter DJ, 2021. How I treat primary ITP in adult patients who are unresponsive to or dependent on corticosteroid treatment. *Blood*, 137(20):2736-2744. <https://doi.org/10.1182/blood.2021010968>
- Guo L, Kapur R, Aslam R, et al., 2018. Antiplatelet antibody-induced thrombocytopenia does not correlate with megakaryocyte abnormalities in murine immune thrombocytopenia. *Scand J Immunol*, 88(1):e12678. <https://doi.org/10.1111/sji.12678>
- He Y, Xu LL, Feng FE, et al., 2018. Mesenchymal stem cell deficiency influences megakaryocytopoiesis through the TNFAIP3/NF- $\kappa$ B/SMAD pathway in patients with immune thrombocytopenia. *Br J Haematol*, 180(3):395-411. <https://doi.org/10.1111/bjh.15034>
- Hernandez-Molina G, Soto-Abraham V, Zamora-Legoff V, et al., 2021. Differential Th follicular cell subsets in minor salivary glands of patients with primary Sjögren's syndrome and systemic lupus erythematosus associated with Sjögren's syndrome. *Clin Exp Rheumatol*, 39(6 Suppl 133):49-56. <https://doi.org/10.55563/clinexprheumatol/yuj21y>
- Iriki H, Takahashi H, Amagai M, 2023. Diverse role of OX40 on T cells as a therapeutic target for skin diseases. *J Invest Dermatol*, 143(4):545-553. <https://doi.org/10.1016/j.jid.2022.11.009>
- Jacquemin C, Schmitt N, Contin-Bordes C, et al., 2015. OX40 ligand contributes to human lupus pathogenesis by promoting T follicular helper response. *Immunity*, 42(6):1159-1170. <https://doi.org/10.1016/j.immuni.2015.05.012>
- Jacquemin C, Augusto JF, Scherlinger M, et al., 2018. OX40L/OX40 axis impairs follicular and natural Treg function in human SLE. *JCI Insight*, 3(24):e122167. <https://doi.org/10.1172/jci.insight.122167>
- Jensen O, Trivedi S, Meier JD, et al., 2022. A subset of follicular helper-like MAIT cells can provide B cell help and support antibody production in the mucosa. *Sci Immunol*, 7(67):eabe8931. <https://doi.org/10.1126/sciimmunol.abe8931>
- Li X, Wang SW, Feng Q, et al., 2019. Novel murine model of immune thrombocytopenia through immunized CD41 knockout mice. *Thromb Haemost*, 119(3):377-383. <https://doi.org/10.1055/s-0038-1677032>
- Liu B, Lin YH, Yan JC, et al., 2021. Affinity-coupled CCL22 promotes positive selection in germinal centres. *Nature*, 592(7852):133-137. <https://doi.org/10.1038/s41586-021-03239-2>
- Liu XG, Hou Y, Hou M, 2023. How we treat primary immune thrombocytopenia in adults. *J Hematol Oncol*, 16:4. <https://doi.org/10.1186/s13045-023-01401-z>
- Mingot-Castellano ME, Bastida JM, Caballero-Navarro G, et al., 2022. Novel therapies to address unmet needs in ITP. *Pharmaceuticals*, 15(7):779. <https://doi.org/10.3390/ph15070779>
- Morita R, Schmitt N, Bentebibel SE, et al., 2011. Human blood CXCR5<sup>+</sup>CD4<sup>+</sup> T cells are counterparts of T follicular cells and contain specific subsets that differentially support antibody secretion. *Immunity*, 34(1):108-121. <https://doi.org/10.1016/j.immuni.2010.12.012>
- Nagashima H, Ishii N, So T, 2018. Regulation of interleukin-6 receptor signaling by TNF receptor-associated factor 2 and 5 during differentiation of inflammatory CD4<sup>+</sup> T cells. *Front Immunol*, 9:1986. <https://doi.org/10.3389/fimmu.2018.01986>
- National Research Council (US) Committee for the Update of the Guide for the Care and Use of Laboratory Animals, 2011. Guide for the Care and Use of Laboratory Animals. 8th Edition. National Academies Press (US), Washington DC. <https://www.ncbi.nlm.nih.gov/sites/books/NBK54049>
- Pedros C, Altman A, Kong KF, 2018. Role of TRAFs in signaling pathways controlling T follicular helper cell differentiation and T cell-dependent antibody responses. *Front Immunol*, 9:2412. <https://doi.org/10.3389/fimmu.2018.02412>
- Pontarini E, Murray-Brown WJ, Croia C, et al., 2020. Unique expansion of IL-21<sup>+</sup> Tfh and Tph cells under control of ICOS identifies Sjögren's syndrome with ectopic germinal centres and MALT lymphoma. *Ann Rheum Dis*, 79(12):1588-1599. <https://doi.org/10.1136/annrheumdis-2020-217646>
- Sasaki T, Bracero S, Keegan J, et al., 2022. Longitudinal immune cell profiling in patients with early systemic lupus erythematosus. *Arthritis Rheumatol*, 74(11):1808-1821. <https://doi.org/10.1002/art.42248>
- Schmitt N, Bentebibel SE, Ueno H, 2014. Phenotype and functions of memory Tfh cells in human blood. *Trends Immunol*, 35(9):436-442. <https://doi.org/10.1016/j.it.2014.06.002>
- Shesternya PA, Savchenko AA, Gritsenko OD, et al., 2022. Features of peripheral blood Th-cell subset composition and serum cytokine level in patients with activity-driven ankylosing spondylitis. *Pharmaceuticals*, 15(11):1370. <https://doi.org/10.3390/ph15111370>
- Sitritn J, Suto E, Wuster A, et al., 2017. The Ox40/Ox40 ligand pathway promotes pathogenic Th cell responses, plasmablast accumulation, and lupus nephritis in NZB/W F1 mice. *J Immunol*, 199(4):1238-1249. <https://doi.org/10.4049/jimmunol.1700608>
- So T, Soroosh P, Eun SY, et al., 2011. Antigen-independent signalosome of CARMA1, PKC $\theta$ , and TNF receptor-associated factor 2 (TRAF2) determines NF- $\kappa$ B signaling in T cells. *Proc Natl Acad Sci USA*, 108(7):2903-2908. <https://doi.org/10.1073/pnas.1008765108>

- Sun CH, Yang J, Wang MZ, et al., 2018. Icaritin improves antibody-induced thrombocytopenia in a mouse model by regulating T-cell polarization. *Planta Med*, 84(3):168-175. <https://doi.org/10.1055/s-0043-119643>
- Vernava I, Schmitt CA, 2023. Daratumumab as a novel treatment option in refractory ITP. *Blood Cells Mol Dis*, 99: 102724. <https://doi.org/10.1016/j.bcmd.2023.102724>
- Vianelli N, Auteri G, Buccisano F, et al., 2022. Refractory primary immune thrombocytopenia (ITP): current clinical challenges and therapeutic perspectives. *Ann Hematol*, 101(5):963-978. <https://doi.org/10.1007/s00277-022-04786-y>
- Victoria GD, Nussenzweig MC, 2022. Germinal centers. *Annu Rev Immunol*, 40:413-442. <https://doi.org/10.1146/annurev-immunol-120419-022408>
- Wang L, Xu L, Hao HY, et al., 2020. First line treatment of adult patients with primary immune thrombocytopenia: a real-world study. *Platelets*, 31(1):55-61. <https://doi.org/10.1080/09537104.2019.1572875>
- Wei XD, Niu XY, 2023. T follicular helper cells in autoimmune diseases. *J Autoimmun*, 134:102976. <https://doi.org/10.1016/j.jaut.2022.102976>
- Xiao X, Balasubramanian S, Liu WT, et al., 2012. OX40 signaling favors the induction of T<sub>H</sub>9 cells and airway inflammation. *Nat Immunol*, 13(10):981-990. <https://doi.org/10.1038/ni.2390>
- Xu Y, Xu HM, Zhen Y, et al., 2019. Imbalance of circulatory T follicular helper and T follicular regulatory cells in patients with ANCA-associated vasculitis. *Mediators Inflamm*, 2019:8421479. <https://doi.org/10.1155/2019/8421479>
- Yang WS, Cui XH, Sun DP, et al., 2023. POU5F1 promotes the proliferation, migration, and invasion of gastric cancer cells by reducing the ubiquitination level of TRAF6. *Cell Death Dis*, 14(12):802. <https://doi.org/10.1038/s41419-023-06332-8>
- Yu YY, Shi YY, Zuo XY, et al., 2018. Progranulin facilitates the increase of platelet count in immune thrombocytopenia. *Thromb Res*, 164:24-31. <https://doi.org/10.1016/j.thromres.2018.02.137>
- Zhao H, Gu ZW, Wang YX, et al., 2022. IL-9 neutralizing antibody suppresses allergic inflammation in ovalbumin-induced allergic rhinitis mouse model. *Front Pharmacol*, 13:935943. <https://doi.org/10.3389/fphar.2022.935943>